

## Research Paper

**Cite this article:** Naoui A, Charlet I, Guerber S, Lugo J, Hellion C, Allain M, Reig B, Perret E, Podevin F (2025) A germanium telluride switch optically controlled with infrared showing over 30k cycles of operation and 32-fs figure-of-merit. *International Journal of Microwave and Wireless Technologies*, 1–8. <https://doi.org/10.1017/S1759078725102195>

Received: 5 July 2024

Revised: 2 August 2025

Accepted: 15 August 2025

### Keywords:


germanium telluride (GeTe); infrared wavelength; optical actuation; optical simulation; phase change material (PCM); RF-switches

**Corresponding author:** Ayoub Naoui;

Email: [ayoub.naoui@cea.fr](mailto:ayoub.naoui@cea.fr)

© The Author(s), 2025. Published by Cambridge University Press in association with The European Microwave Association. This is an Open Access article, distributed under the terms of the Creative Commons Attribution licence (<http://creativecommons.org/licenses/by/4.0>), which permits unrestricted re-use, distribution and reproduction, provided the original article is properly cited.

# A germanium telluride switch optically controlled with infrared showing over 30k cycles of operation and 32-fs figure-of-merit

Ayoub Naoui<sup>1</sup> , Ismael Charlet<sup>2</sup>, Sylvain Guerber<sup>2</sup>, Jose Lugo<sup>2</sup>, Clemence Hellion<sup>2</sup>, Marjolaine Allain<sup>2</sup>, Bruno Reig<sup>2</sup>, Etienne Perret<sup>1</sup> and Florence Podevin<sup>1</sup>

<sup>1</sup>Grenoble INP-UGA, Grenoble, France and <sup>2</sup>University Grenoble Alpes, CEA, Leti, Grenoble, France

## Abstract

This article presents germanium telluride (GeTe)-based switches for radiofrequency (RF) applications, capable of reversible switching between their ON and OFF states through optical activation by irradiation. Unlike previous studies, the transition is induced by infrared laser pulses at a wavelength of  $\lambda = 915$  nm, which is highly promising for future integration of laser sources and the proposal of fully integrated optical activation of phase change material (PCM) switches. This represents a novel approach compared to the existing literature, which primarily focuses on the ultra-violet spectrum, less suitable for on-chip optical integration. Our work also provides combined optical and thermal simulations to elucidate the challenges associated with actuating small PCM switches and demonstrates the effectiveness of PCMs at this wavelength. The study achieves bistable switching at high frequencies up to 40 GHz, with a figure of merit of 31.5 fs, despite the low GeTe conductivity of only  $1.85 \cdot 10^5$  S/m. Additionally, significant advancements over the literature have been made by surpassing 30,000 cycles with optical actuation.

## Introduction

Phase change materials (PCM) have a long history of application, mainly in the field of non-volatile memories [1] and the optical storage industry [2]. Beyond these traditional applications, PCMs have also found a variety of uses in integrated photonics [3]. Recently, chalcogenide PCMs, particularly germanium telluride (GeTe) and germanium-antimony-telluride, have emerged as promising materials for the design of next-generation radiofrequency (RF) switches. These switches exploit the unique properties of PCMs, such as their ability to phase shift between amorphous and crystalline states, enabling rapid and reversible transitions with significant effects on the electrical characteristics of the device. RF switches based on PCMs offer several notable advantages. First, they can handle high power levels while maintaining a low resistance-capacitance product ( $R_{ON}C_{OFF}$ ), which is crucial for the performance of RF circuits. Second, these switches are non-volatile, meaning they retain their switching state even in the absence of power supply, thereby reducing power consumption and increasing system reliability [4]. Third, their low power consumption makes them particularly suitable for applications where energy efficiency is essential. These characteristics make PCM-based RF switches indispensable for modern RF technologies, which must meet very interesting for stringent performance and efficiency requirements. For instance, in millimeter-wave radar systems, the ability of switches to handle high frequencies with minimal losses is crucial for improving radar resolution and range. Similarly, 6G communication networks, aiming to deliver ultra-fast data transmission speeds and extremely low latency, can benefit from the integration of PCM switches to optimize RF circuit performance [5–7].

However, the activation of these PCM-based RF switches presents significant challenges. Conventional methods often rely on indirect heating using micro-heaters, which generate heat through the Joule effect [8]. This can lead to considerable parasitic capacitance, thereby limiting RF performance. Additionally, the non-uniform temperature distribution between the micro-heater and the PCM element can adversely affect the RF performance [9]. Incomplete crystallization or amorphization of the PCM can result in increased  $R_{ON}$  or  $C_{OFF}$ , thus degrading the switch cutoff frequency. Alternative solutions, such as optical actuation, have been explored [10–12]. These methods leverage the strong optical absorption of GeTe at specific wavelengths, allowing the conversion of optical energy into heat to switch the PCM for various applications. For instance, optically controlled GeTe has been used to reconfigure band-stop filters and polarizers in the THz frequency range [12]. A reconfigurable antenna utilizing GeTe deposits to

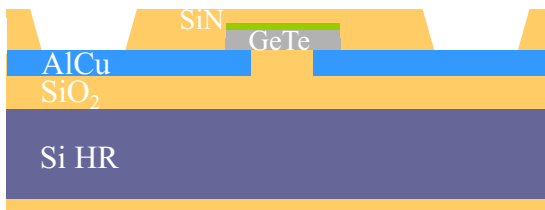


Figure 1. Switch stacking structure.

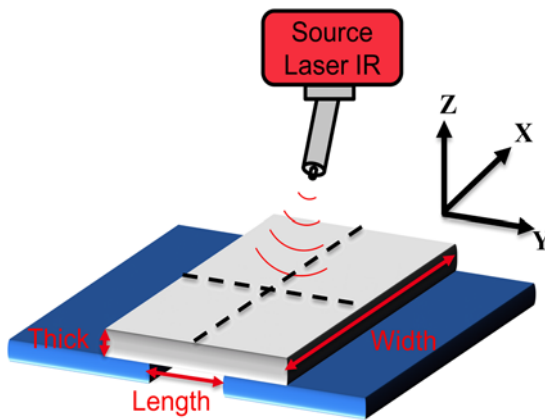


Figure 2. 3D simulation setup.

connect or disconnect radiating elements is presented in [10]. Furthermore, [11] demonstrates a large-scale RF-PCM switch, with performance characterized by frequency. Nevertheless, these approaches have been hampered by the use of expensive UV lasers that are not compatible with current CMOS integrated photonics technology. In contrast, a wavelength of 915 nm, which is the standard for integrated photonic circuits, offers a promising alternative [13, 14]. This wavelength allows for the use of low-cost, chip-scale pulsed lasers that can be easily integrated into a photonic chip.

Therefore, studying the actuation of RF PCM switches at 915 nm offers a compelling solution to the aforementioned challenges and paves the way for PCM/photonic co-integration. An earlier version of this paper was presented at EuMW 2024 and was published in its Proceedings [24]. In this context, this work presents, to the best of our knowledge, the first combined thermo-optical simulations of GeTe RF switches to highlight the issues in actuating small switches, as well as to study their optical actuation performance at an IR wavelength of 915 nm and the confirmation of those results by measurements. It should be noted that power handling measurements have already been performed on similar switches in previous work reported in [23]. The first part of this work describes the technological stack of our GeTe RF switches and the results of combined optical and thermal simulations. The second part details the conditions for optical actuation at 915 nm and the measured results that include DC and RF performances and endurance testing. The final part provides a comparison with the state-of-the-art.

## Optical actuation of GeTe material

### Technology and test bench description

In this study, RF switches in a Single Pole Single Throw (SPST) configuration are integrated on a coplanar waveguide utilizing GeTe, with a Ge[50%]:Te[50%] target. The GeTe is deposited at a low temperature and subsequently annealed to achieve an initial crystalline state. The switch stacking structure is shown in Figure 1. The developed process flow ensures compatibility with standard CMOS back-end-of-line processes and meets the performance requirements of PCM switches. Using this technological framework, we have developed a 3D simulation setup for the optical actuation of our switches, as illustrated in Figure 2. In this setup, two RF lines are connected by a GeTe segment, parameterized by its width (X), length (RF gap) (Y), and thickness (Z). An optical wave source with a Gaussian profile is positioned 10  $\mu\text{m}$  above the GeTe to induce phase transitions between the crystalline (ON) and amorphous (OFF) states. This transition is accomplished by heating the GeTe

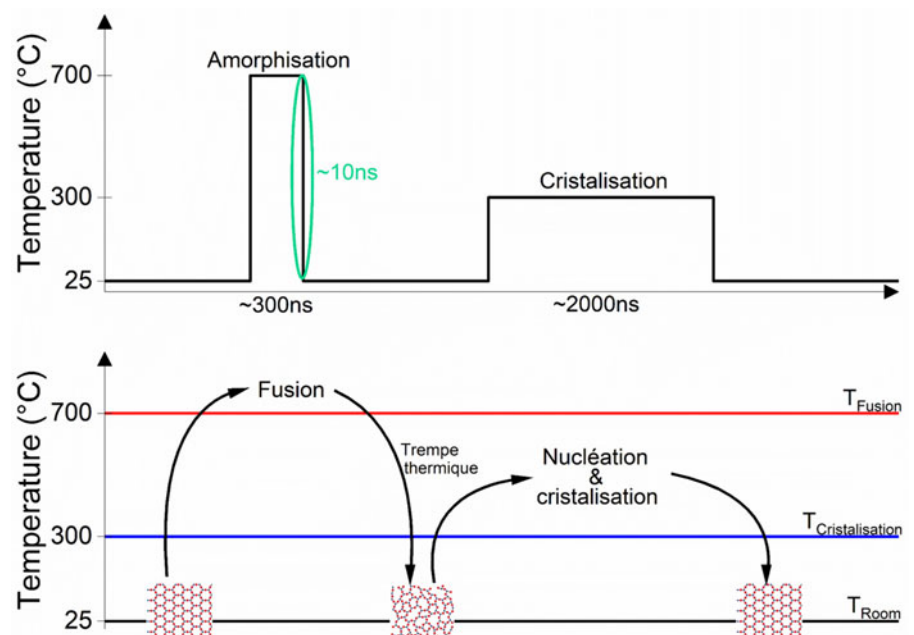
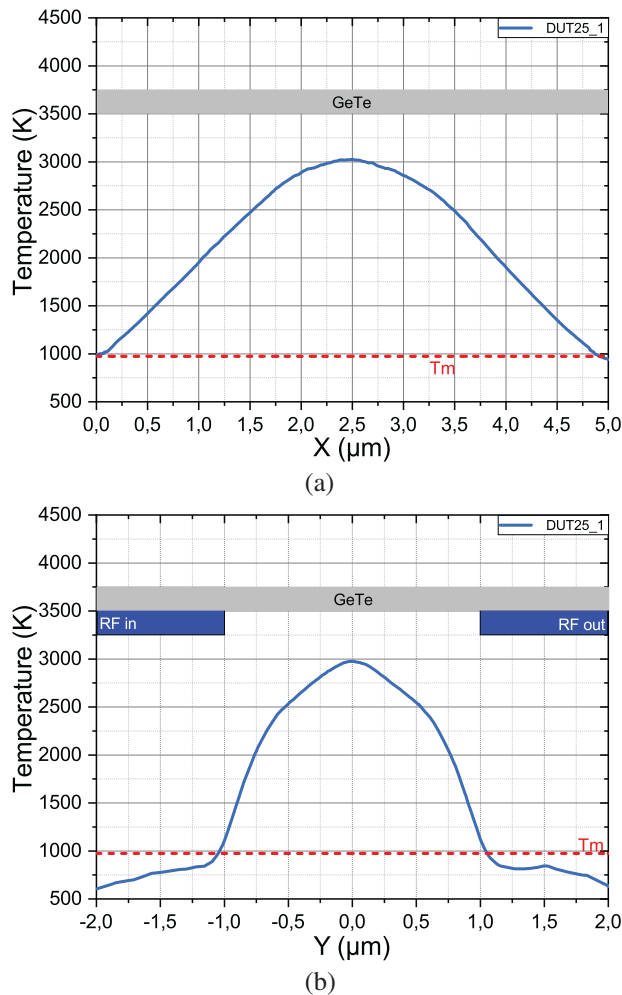


Figure 3. Reversible switching of a phase-change material using an optical pulse.



**Figure 4.** Temperature variation according to: (a) PCM length and (b) PCM width.

above its melting temperature ( $T_m \sim 973$  K) for a brief period, followed by rapid quenching to solidify the atoms in the amorphous state, as shown in Figure 3. Crystallization is achieved by applying a pulse of longer duration (2  $\mu$ s), which heats the PCM above its recrystallization temperature ( $T_c \sim 573$  K), thereby activating crystal grain growth and nucleation. This process changes the resistivity of the PCM from the amorphous (high resistivity) to the crystalline (low resistivity) state.

### Optical and thermal coupled simulation

Optical and thermal simulations were conducted using ANSYS Lumerical software, employing a Gaussian source of 5  $\mu$ m diameter to irradiate the PCM with a power of 300 mW and a duration of 300 ns. Initially, a simulation was performed using the FDTD solver to calculate the optical power absorbed per unit volume due to the material absorption, which is then integrated over the entire volume of the GeTe to obtain the total absorption. This parameter is subsequently transferred to the HEAT solver to import the optical absorption data and use it as a heat source in the simulation. The graphs in Figure 4 illustrate the temperature evolution of GeTe as a function of its width and length, recorded on the monitors (represented as a dashed line in Figure 2). Notably, the critical temperature required for GeTe amorphization is exceeded in the

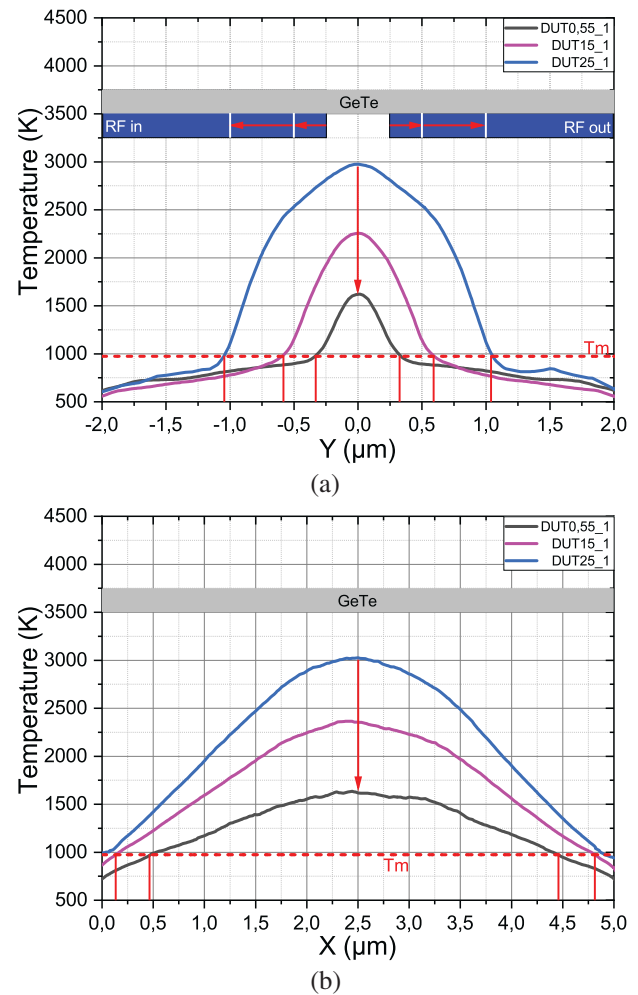


**Figure 5.** Temperature variation for different RF gaps depending on: (a) PCM length and (b) PCM width.

**Table 1.** Different devices of GeTe studied in this work

Name	PCM length	PCM width	PCM thick	Optical fiber
DUT0.55_1	0.5 $\mu$ m	5 $\mu$ m	100 nm	Hi 780 $\varnothing$ 5 $\mu$ m
DUT15_1	1 $\mu$ m	5 $\mu$ m	100 nm	Hi 780 $\varnothing$ 5 $\mu$ m
DUT25_1	2 $\mu$ m	5 $\mu$ m	100 nm	Hi 780 $\varnothing$ 5 $\mu$ m
DUT15_2	1 $\mu$ m	5 $\mu$ m	200 nm	Hi 780 $\varnothing$ 5 $\mu$ m
DUT25_2	2 $\mu$ m	5 $\mu$ m	200 nm	Hi 780 $\varnothing$ 5 $\mu$ m

Note: Hi780 : high index fiber with operating  $\lambda$  of 780 nm.

structure with a 5  $\mu$ m width and a 2  $\mu$ m RF gap, as indicated by the temperature surpassing the melting threshold over the entire width of our GeTe.

Using the same structure and energy input, we varied the RF gap. The results, illustrated in Figure 5(a) and (b), where the nomenclature stands for Device Under Test with an RF gap varying between 0.5 and 2  $\mu$ m in X, a width of 5  $\mu$ m in Y and a thickness of 100 nm in Z, indicate that decreasing the RF gap significantly enhances heat dissipation towards the metallic contacts (RF pads). This is evident from the 1500 K temperature drop observed at the center of the GeTe between structures DUT25\_1 and DUT0.55\_1. The increased thermal dissipation complicates

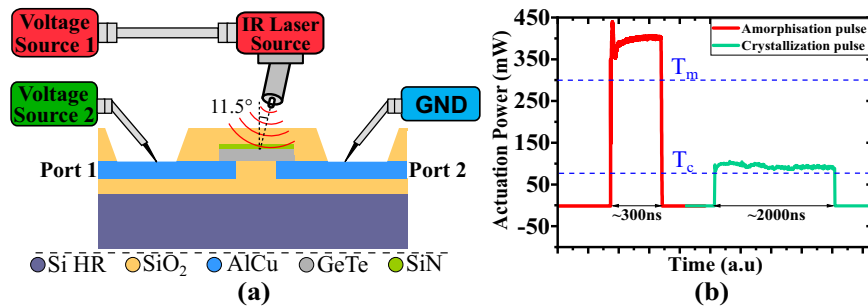


**Figure 6.** (a) Experimental setup for measurement; (b) Example of laser pulses used in this work.

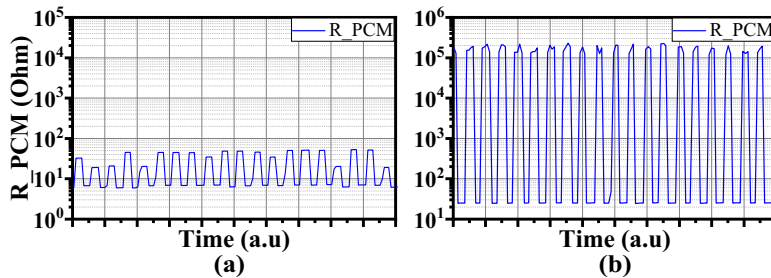


**Figure 7.** Resistance computation results for different GeTe lengths: (a) For 0.5  $\mu\text{m}$  of length; (b) For 2  $\mu\text{m}$  of length.

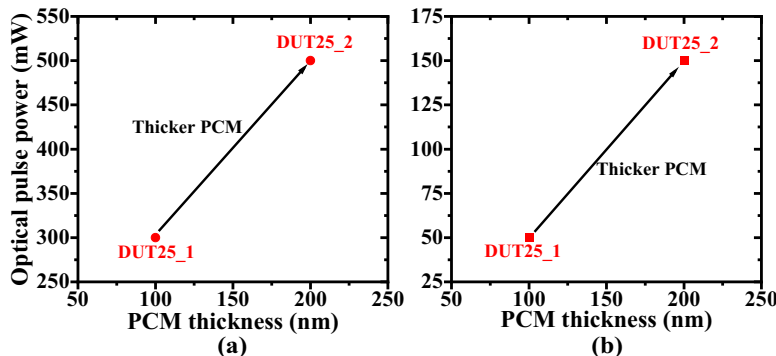


**Figure 8.** Optical pulse power to amorphize (a) and crystallize (b) PCMs of various thicknesses of 100 and 200 nm, respectively.

the switching of smaller gaps, as parts of the PCM do not reach the melting temperature due to the proximity of the metal, which has a much higher thermal conductivity than GeTe. This highlights the difficulty of achieving a complete phase change in structures with smaller RF gaps, as will be demonstrated in the subsequent measurement section.

## Measurement results

### Optical command optimization

Upon completion of the optical and thermal simulations, the RF switches were tested using GeTe samples of various lengths and thicknesses, as summarized in Table 1. Optical activation was performed by direct irradiation using an optical fiber connected to a pulsed laser source (915LD-1-3-2) operating at a wavelength of 915 nm. The fiber is positioned 10  $\mu\text{m}$  above the PCM element, with an incidence angle of 11.5° relative to the surface normal, as illustrated in Figure 6(a). A Hi780 optical fiber with a diameter of 5  $\mu\text{m}$  is used to match the width of the 5  $\mu\text{m}$  switches. Micro-positioners from a standard Cascade automatic probing station enable precise alignment of the fiber with the PCM at the wafer level, allowing the delivery of a Gaussian light energy that is tunable and highly localized to the PCM switches. These light pulses are absorbed by the material, causing localized heating within the

PCM. The resulting temperature increase, followed by cooling, induces a phase transition in the PCM, thereby altering its optical and electrical properties, especially its resistance. The devices are actuated with two types of optical pulses, as shown in Figure 6(b). A powerful, short pulse ( $\sim 300$  ns) for amorphization and a less powerful, longer pulse ( $\sim 2000$  ns) for crystallization. To extract the DC resistance of the PCM, a two-probe measurement technique is used by applying a 10 mV pulse with a Keithley B2902A source, after each optical activation. Figure 7 illustrates the variation in DC resistance between the amorphous and crystalline states after each pulse. It is observed that with a switch having a 0.5  $\mu\text{m}$  RF gap (Figure 7(a)), the switching of GeTe fails, with an  $R_{\text{OFF}}/R_{\text{ON}}$  ratio below 20. This failure is attributed to the partial amorphization of GeTe, which does not reach its melting temperature uniformly because of the Gaussian intensity distribution and the high heat dissipation from the metal (RF pads) closer to the center of the GeTe. Conversely, with a switch having a 2  $\mu\text{m}$  RF gap, the GeTe switches correctly, achieving an  $R_{\text{OFF}}/R_{\text{ON}}$  ratio exceeding  $10^4$ , as shown in Figure 7(b). These results confirm the findings from our combined optical and thermal simulations. Figure 8 illustrates the minimum power required to amorphize the DUT25\_1 and DUT25\_2 devices when optical pulses with increments of 50 mW are applied until switching is achieved. It is noteworthy that the switches are illuminated by a 5  $\mu\text{m}$  fiber with an almost Gaussian profile, indicating that the light is localized at the center.



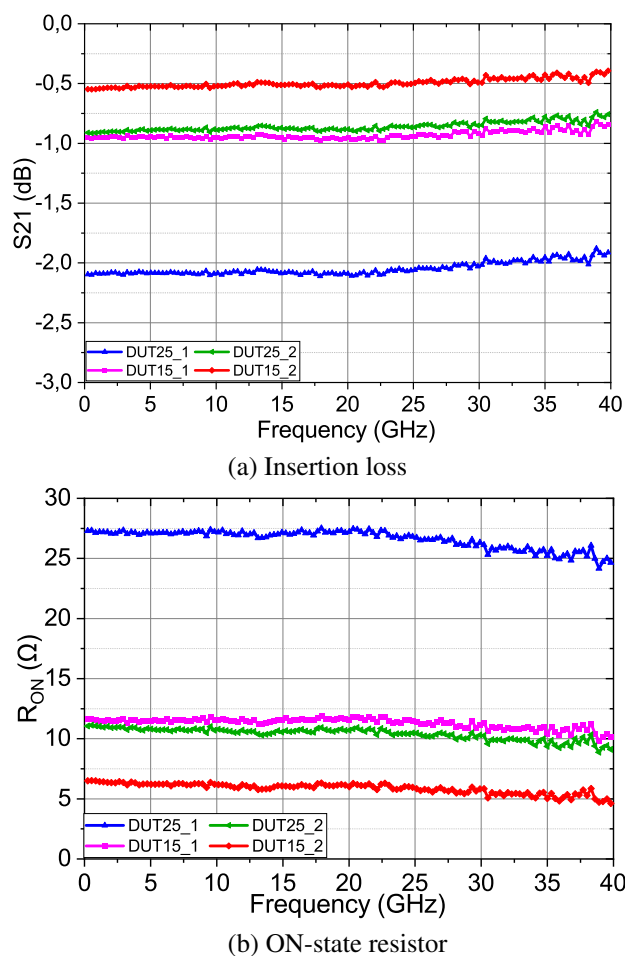


Figure 9. Crystalline GeTe RF performances for different sizes.

To ensure sufficient temperature at the edges of the sample, the comparison between DUT25\_1 and DUT25\_2 highlights the effect of thickness. It is evident that the required switching powers are not proportional to the GeTe volume. Specifically, DUT25\_2, which has twice the volume of GeTe compared to DUT25\_1, requires more than twice the power for switching (Figure 8(a)). This can be explained by the fact that optical absorption follows an exponential decay with thickness. Figure 8(b) leads to similar conclusions for the crystallization process.

### RF measurement

The RF performance of optically actuated SPST PCM switches was evaluated through S-parameter measurements performed on all devices using a Keysight PNAX vector network analyzer with two ports. Calibration was conducted over the frequency range of 40 MHz to 40 GHz. Initially, the analysis focused on switches in the ON state (optically crystallized PCM). Figure 9(a) illustrates the measured insertion loss after de-embedding in this state for switches of various lengths and thicknesses. The observations indicate that the insertion loss is halved by either doubling the PCM cross-sectional area or halving its length. These results are subsequently used to extract the on-state resistance ( $R_{ON}$ ) up to 40 GHz, as shown in Figure 9(b). This figure highlights the reduction in resistance from 12  $\Omega$  (DUT15\_1) to 6  $\Omega$  (DUT15\_2)

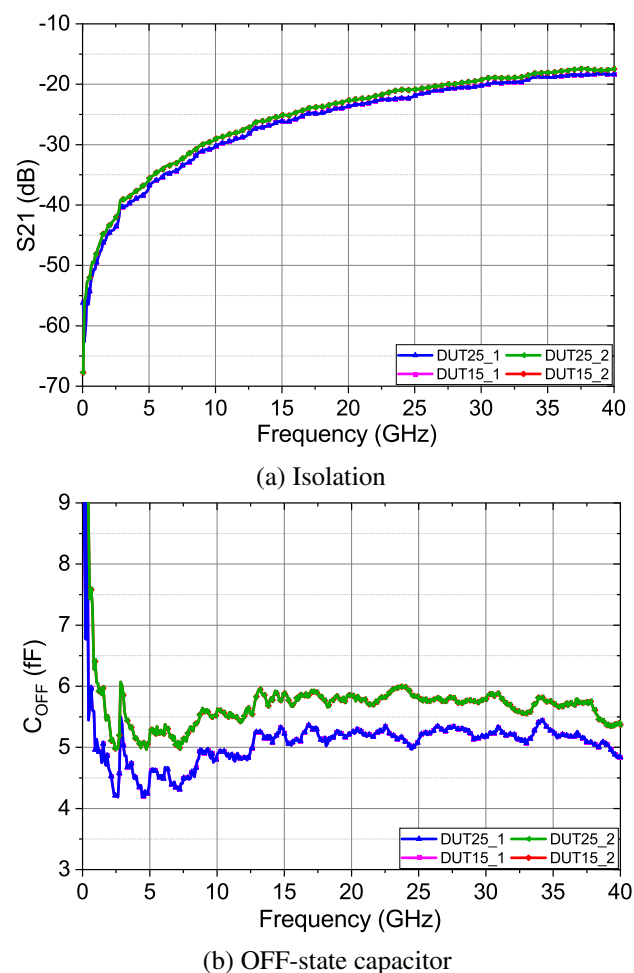


Figure 10. Amorphous GeTe RF performances for different sizes.

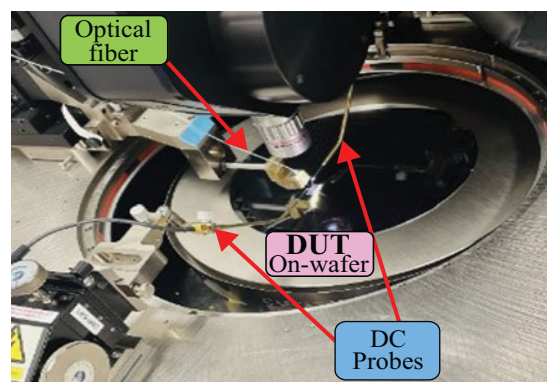
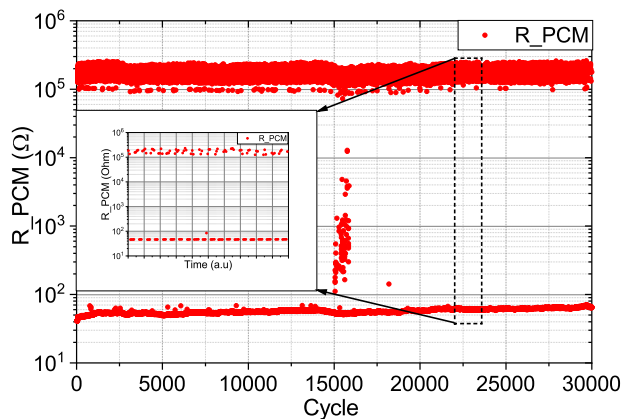


Figure 11. Photograph of the optical measurement test bench on the wafer.

when the cross-sectional area of the PCM switch is doubled while maintaining the same length of 1  $\mu\text{m}$ . This outcome corroborates the theoretical calculations presented in Table 2, emphasizing the advantages of thicker PCM layers. Figure 10(a) displays the S-parameters of the switches in the OFF state. In this scenario, the SPST switches are optically actuated by a short pulse to achieve the amorphous state, characterized by an excellent isolation exceeding 19 dB across the entire frequency range up to 40 GHz. The OFF-state capacitances are extracted and presented in Figure 10(b).



**Figure 12.** Switching cycles measurement.

As anticipated, the thicker devices exhibit slightly higher capacitances (but no more than 0.8 fF of additional capacitance) due to the doubled coupling area. This results in a figure of merit ( $\text{FoM} = R_{\text{ON}} \cdot C_{\text{OFF}}$ ) of 31.5 fs with a cutoff frequency of 5 THz for device DUT15\_2, compared to 57.9 fs and 2.75 THz for device DUT15\_1.

### Cycling

After determining the conditions for optical actuation, the switching cycle is studied on a switch with a length of 4  $\mu\text{m}$ , a width of 5  $\mu\text{m}$  and a thickness of 100 nm. Using the configuration of Figure 11, applying laser pulses (one for amorphization, then one for crystallization) with a repetition rate of 4 Hz as in Figure 6(b), the DC resistance was measured over several hours for both states after each transition, as shown in Figure 12. DC resistance is plotted as a function of the number of cycles, demonstrating that 30k cycles are achieved with an  $R_{\text{OFF}}/R_{\text{ON}}$  ratio greater than  $10^4$ . Moreover, the crystalline and amorphous DC resistance values remain stable throughout the measurements, indicating that the cycling process is conducted effectively. However, some OFF-state DC resistance

values are observed below  $10^5 \Omega$ , suggesting that GeTe did not fully amorphize as expected. Specifically, 30 failed amorphization pulses are counted. These PCM amorphization failures are due to micro-vibrations of the positioners caused by external elements that temporally misaligning the fiber, leading to partial amorphization of the PCM. Nevertheless, this did not cause any degradation to our switch. Despite these measurement limitations, this represents the first demonstration of an optically actuated PCM switch with such a high number of cycles, whereas only a dozen of cycles have been achieved so far [10, 12].

### Discussion

Table 2 compares the endurance of the switching cycles and the FoM of our work with those published in the literature, considering both indirect electrical and optical excitations at a wavelength of 248 nm, which is incompatible with current integrated photonic technology. Regarding the optical excitation, significant performance can be observed in terms of switching cycles. As previously mentioned, this is the first time such a high number of cycles has been achieved with optical excitation, compared to [10, 12]. A FoM of 31.5 fs is obtained, which is comparable to the state of the art, with only 5.5 fs more than in [11], despite their GeTe being ten times larger (even if 3 times longer, this goes in favor of low  $R_{\text{ON}}$ ) and having twice the conductivity of ours. Furthermore, the optical wavelength of 248 nm used in the literature presents particular challenges for integrated photonic, such as material selection, complexity, and manufacturing costs, thus limiting their development, which is not the case for 915 nm. In terms of comparison with electrical excitation, we achieve fewer cycles than [14, 17, 18]. This is due to external factors such as fiber misalignment after hours of cycling, as we did not observe any degradation of our PCM. Comparing the FoM, we can see that our devices present a FoM comparable to the state of the art and also better than our devices with electrical excitation having the same dimensions and GeTe properties, improving from 45.5 to 36 fs for DUT19\_1. This can be explained by the excellent control of the crystalline region during optical excitation, as well as the absence of any heating element that induces parasitic capacitances, making  $C_{\text{OFF}}$  lower.

**Table 2.** Performance comparison with the state-of-the-art

Ref	Actuation	PCM size	PCM thick	$R_{\text{ON\_meas}} (\Omega)$	$R_{\text{ON\_cal}} (\Omega)$	$C_{\text{OFF}} (\text{fF})$	FoM meas (fs)	Cycling
[10]	Optical	$2 \times 5 \mu\text{m}^2$	100 nm	23	–	13.79	–	10
[11]	Optical 248nm	$3 \times 50 \mu\text{m}^2$	200 nm	3	–	8.8	26	–
[12]	Optical 248nm	$1.5 \times 0.5 \text{ mm}^2$	500 nm	–	–	–	–	10
[6]	Electrical	$0.9 \times 30 \mu\text{m}^2$	– nm	0.9	–	14.1	12.7	–
[15]	Electrical	$2 \times 10 \mu\text{m}^2$	75 nm	4.5	–	35	149	–
[16]	Electrical	$5 \times 44 \mu\text{m}^2$	150 nm	11.5	–	3.3	37	300k
[17]	Electrical	$0.6 \times 12 \mu\text{m}^2$	250 nm	3.9	–	10.2	39.8	–
[18]	Electrical	$3 \times - \mu\text{m}^2$	– nm	4.5	–	5.6	25.2	10M
[19]	Electrical	$- \times 10 \mu\text{m}^2$	– nm	2.3	–	2.7	6.2	1B
This work	Electrical	$1 \times 9 \mu\text{m}^2$	100 nm	6.5	$3.8^a$	7	45.5	–
This work	Optical 915nm	$1 \times 9 \mu\text{m}^2$	100 nm	6.11	$3.8^a$	5.9	36	$\approx 30\text{k}$
This work	Optical 915nm	$1 \times 5 \mu\text{m}^2$	200 nm	6	$3.5^a$	5.25	31.5	$\approx 30\text{k}$

<sup>a</sup>Calculated on the basis of the conductivity of [10], which equals to  $2.9 \cdot 10^5 \text{ S/m}$ .

## Conclusion

The optical actuation of an RF switch based on GeTe with various geometries has been studied at a wavelength of 915 nm. The switching conditions for the ON and OFF states have been determined. A cycling test demonstrated a switching capability of at least 30k cycles, representing the highest optical switching rate of PCM switches reported so far. Small signal measurements show a lower FoM for thicker and shorter switches due to their low on-state resistance, confirming the advantage of thicker PCMs under direct optical irradiation. This work paves the way for the realization of high-performance optically actuated RF switches, fully leveraging CMOS-integrated photonics, which will enhance switch performance by eliminating external factors that may affect their performance. Generally, integrated photonics at 915 nm relies on a standard process using silicon nitride optical waveguides [13, 14, 20]. In this context, the co-integration of RF PCM switches and passive integrated photonics represents a significant advancement in optical actuation [21]. Ultimately, the realization of a fully integrated optical actuation circuit can be envisaged using hybrid integrated lasers [22].

**Acknowledgements.** The authors would like to thank all the engineers and technicians involved in cleanroom, DC, RF and photonics characterization, for their contribution to this work.

**Funding statement.** The authors acknowledge financial support through the Presidency of Grenoble Institute of Technology of the University Grenoble Alps and the French Public Authorities within the frame of IPCEI/Nano2022 project.

**Competing interests.** The author(s) declare none.

## References

1. Fantini A, L Perniola, M Armand, JF Nodin V Sousa, A Persico, J Cluzel, C Jahan, S Maitrejean, S Lhostis, A Roule, C Dressler, G Reimbold, B De Salvo, P Mazoyer, D Bensahel and F Boulanger (2009) Comparative assessment of GST and GeTe materials for application to embedded phase-change memory devices 2009 *IEEE International Memory Workshop*. pp. 1–2. Monterey, CA, USA.
2. Ovshinsky SR. (1968) Reversible electrical switching phenomena in disordered structures. *Physical Review Letters*. 21, 1450–1453
3. Wang X, H Qi, X Hu, Z Yu, S Ding, Z Du and Q Gong. (2021) Advances in photonic devices based on optical phase-change materials. *Molecules Journal* 26, 2813
4. Naoui A, B Reig, E Perret, M El-Chaar and F Podevin. (2023). Indirect electrical-control through heating of a GeTe phase change switch and its application to reflexion type phase shifting 2023 *International Microwave and Antenna Symposium*, Egypt, pp. 13–16.
5. Singh T and RR Mansour. (2019). Miniaturized DC–60 GHz RF PCM GeTe-based monolithically integrated redundancy switch matrix using T-Type switching unit cells. 2019 *IEEE Transactions on Microwave Theory and Techniques*, IEEE, pp. 5181–5190
6. El-Hinnawy N, P Borodulin, EB Jones, BP Wagner, MR King, JS Mason, J Bain, J Paramesh, TE Schlesinger, RS Howell, MJ Lee and RM Young. In (2014). THz Fco GeTe inline phase-change switch technology for reconfigurable RF and switching applications. 2014 *IEEE Compound Semiconductor Integrated Circuit Symposium*, IEEE, CA, USA, pp. 1–3.
7. Wainstein N, G Adam, E Yalon and S Kvatsinsky. (2021) Radiofrequency switches based on emerging resistive memory technologies - A survey. *Proceedings of the IEEE* 109, 77–95
8. Gharbieh S, A Clemente, J Milbrandt and B Reig. (2022). Phase change material based reconfigurable transmitarray: a feasibility study 2022 *16th European Conference on Antennas and Propagation (EuCAP)*, IEEE, Madrid, Spain, pp. 1–4.
9. Charlet I *et al.* (2022). RF performance of large germanium telluride switches for power application 18th *European Microwave Integrated Circuits Conference (EuMIC)*, IEEE, Berlin, Germany, pp. 177–180
10. Chau L, G James, X Lan, G Altvater, RM Young, N El-Hinnawy, D Nichols J Volakis and N Ghalichechian. (2015) Optically controlled gete phase change switch and its applications in reconfigurable antenna arrays. *SPIE Defense and Security* 9479, 947905
11. Crunteanu A, L Huitema, J-C Orlianges, C Guines and D Passerieux. (2017). Optical switching of GeTe phase change materials for high-frequency applications 2017 *IEEE MTT-S International Microwave Workshop Series on Advanced Materials and Processes for RF and THz Applications*, IEEE, Pavia, Italy, pp. 1–3.
12. Pinaud M, G Humbert, S Engelbrecht, L Merlat, BM Fischer and A Crunteanu 2021. Terahertz devices using the optical activation of GeTe phase change materials: toward fully reconfigurable functionalities. *ACS Photonics* 8, 3272–3281
13. Qiu Y *et al.* (2019). Ultra-High-Power and High-Efficiency 905nm Pulsed Laser for LiDAR. 2019 *IEEE 4th Optoelectronics Global Conference (OGC)*, IEEE, Shenzhen, China, pp. 32–35.
14. Monfray S *et al.* (2022). Optical Phased Array for 905-nm LIDAR applications integrated on 300mm Si-Photonic Platform 2022 *Optical Fiber Communications Conference and Exhibition (OFC)*, IEEE, CA, USA, pp. 1–3.
15. El-Hinnawy N *et al.* (2013) A four-terminal, inline, chalcogenide phase-change RF switch using an independent resistive heater for thermal actuation. *IEEE Electron Device Letters* 34, 1313–1315
16. Moon J, H Seo, K Son, K Lee, D Zehnder, H Tai and D Le. (2018). Phase-change RF switches with robust switching cycle endurance 2018 *IEEE Radio and Wireless Symposium*, IEEE, CA, USA, pp. 231–233.
17. Wang M and M Rais-Zadeh. (2014). Directly heated four-terminal phase change switches 2014 *IEEE MTT-S International Microwave Symposium*, IEEE, FL, USA, pp. 1–4.
18. Moon J, KS Hwa-change Seo, DZ Kangmu Lee and H Tai. (2018). 5 THz figure-of- Merit reliable phase-change RF switches for millimeter-wave applications 2018 *IEEE/MTT-S International Microwave Symposium*, IEEE, PA, USA, pp. 836–838.
19. El-Hinnawy N, G Solvin, J Rose and D Howard. (2020). A 25 THz  $F_{CO}$  (6.3 fs  $R_{ON}C_{OFF}$ ) phase-change material RF switch fabricated in a high volume manufacturing environment with demonstrated cycling > 1 billion times 2020 *IEEE/MTT-S International Microwave Symposium*, IEEE, CA, USA, pp. 45–48.
20. Marinins A, S Hansch, H Sar, F Chancerel, N Golshani, H-L Wang, A Tsiara, D Coenen, P Verheyen, G Capuz, Y De Koninck, O Yilmaz, G Morthier, F Schleicher, G Jamieson, S Smyth, A McKee, Y Ban, M Pantouvaki, C La Tulipe Douglas and J Van Campenhout. (2023). Wafer-scale hybrid integration of InP DFB lasers on Si photonics by flip-chip bonding with sub-300 nm alignment precision 2023 *IEEE Journal of Selected Topics in Quantum Electronics*. 1–11
21. Reig B, C Hellion, I Charlet, M Allain and A Naoui. (2025). Phase-change material switch. *US Patent App.* 18/787,124
22. Tyler N, D Fowler, S Malhouitre, S Garcia, P Grosse, W Rabaud and B VSzelag. (2019) SiN integrated optical phased arrays for two-dimensional beam steering at a single near-infrared wavelength. *Optics Express* 27, 5851–5858
23. Charlet I, S Guerber, A Naoui, B Charbonnier, C Dupré, J Lugo, C Hellion, M Allain, F Podevin, E Perret and B Reig. (2023) Optical actuation performance of phase-change RF switches. *IEEE Electron Device Letters* 45, 500–503
24. Naoui A, S Guerber, I Charlet, B Charbonnier, C Dupré, J Lugo, C Hellion, M Allain, B Reig, E Perret and F Podevin. (2024). Optical actuation of GeTe phase-change RF switches at 915nm: performance comparison for different GeTe sizes and impact of cycling 2024 *19th European Microwave Integrated Circuits Conference*, IEEE, Paris, FRANCE, pp. 218–221.





**Ayoub Naoui** received the master's degree in wireless integrated circuits and systems from the University of Grenoble Alpes, Grenoble, France, in 2021. He is currently pursuing the Ph.D. degree in TIMA Laboratory and CEA-Leti, Grenoble. His research interests include integrated optical actuation of RF switches based on phase change materials and integration on millimeter wave circuits.



**Ismael Charlet** received the M.Sc. degree in nanotechnologies from Grenoble-INP Phelma, France, in 2017, and the Ph.D. degree in optoelectronics & photonics from the University of Paris-Saclay, France, in 2021. He is currently a researcher with CEA-Leti, France.



**Sylvain Guerber** received the M.Sc. degree in nanotechnologies from the Paris-Sud University, Saclay, France, the Engineering degree in embedded electronics from the ECE Engineering School, Paris, France, and the Ph.D. degree in optoelectronics and photonics from the University of Paris-Saclay, France, in 2019. He is currently a researcher with CEA-LETI, Grenoble, France. His research interests include silicon photonics devices and circuits, non-linear optical devices & integrated lasers.



**Jose Lugo-Alvarez** received the Ph.D. degree in Radio Frequency from the University of Grenoble Alpes, France, in 2015. He is currently an RF Research Engineer with CEA-LETI, Grenoble, France. His current research interests include small- and large-signal characterization, modeling, and the optimization of active devices and semiconductor substrates toward RF applications in CMOS advanced technologies.



**Clemence Hellion** received her bachelor's degree in chemistry. She joined CEA Leti in 2012, as a manufacturing process specialist, where she worked on RF components. Since 2021, her research has focused on manufacturing processes for RF switches based on phase-change materials.



**Marjolaine Allain** received a master's degree in physical sciences and a diploma in applied technical research (DRT) focusing on the ship design and manufacturing laboratory, from Grenoble-INP, ENSPG, in 2007 and 2009, respectively. She joined CEA-LETI in 2010 to develop manufacturing processes for sensors and actuators (MEMS) designed with piezoelectric materials. After a few years devoted to micro-battery applications, she

joined the RF laboratory to work on passive components and PCM switches.



**Bruno Reig** received the Ph.D. degree in electronics from Pierre & Marie Curie University, Paris, France, in 1999. From 1995 to 2004, he was a Research Engineer with Thales Research & Technology, Palaiseau, France, where he was involved in the development of advanced packaging solutions for microwave modules. In 2004, he joined the MicroSystem Components Section, CEA LETI, Grenoble, France, where he was implied in the design, realization and characterization of RF MEMS switches and NEMS sensors. He also participated in the development of integrated mmW circuits design on advanced CMOS SOI technology. He is also a CEA Expert and a Project Manager in RF components and packaging solutions with CEA LETI.



**Etienne Perret** received the Ing. degree in electrical engineering from the ENSEEIHT, Toulouse, France, in 2002, and the M.Sc. and Ph.D. degrees in electrical engineering from the Toulouse Institute of Technology, Toulouse, in 2002 and 2005, respectively. From 2005 to 2006, he held a post-doctoral position with the Institute of Fundamental Electronics, Orsay, France. Since 2006, he has been an Associate Professor of electrical engineering with Grenoble Alpes University

– Grenoble Institute of Technology, Grenoble, France. Since 2014, he has been a Junior Member with the University Institute of France, Paris, France, an institution that distinguishes professors for their research excellence, as evidenced by their international recognition. He has authored or coauthored more than 150 technical conferences, letters, journal articles, books, and book chapters. His current research interests include the electromagnetic modeling of passive devices for millimeter and submillimeter-wave applications, and wireless communications, especially RFID and chipless RFID.



**Florence Podevin** received the B.Eng. degree in electronics and microelectronics from the École Centrale de Lille, Villeneuve-d'Ascq, France, in 1998, and the M.Sc. degree in electronics and microelectronics and the Ph.D. degree in microelectronics from the Université des Sciences et Technologies de Lille (USTL), in 1998 and 2001, respectively. In 2001, she joined the "Institute of Microelectronics, Electromagnetism and Photonics," Grenoble, France, as an Assistant

Professor. She is currently a Professor with the Laboratory "Techniques of Informatics and Microelectronics for integrated systems Architecture," Grenoble. She has authored or coauthored more than 160 papers published in international journals and national or international conferences and co-holds four patents. Her main research interests concern low-power RF and millimeter-wave architectures with codesign between passive and active devices, performing integrated distributed and lumped passive elements. She is also involved with the co-integration of spintronics devices or phase change material-based switches with microelectronics.